Solvation of Yttrium with Ammonia: An Experimental and Theoretical Study

Benoit Simard,* David M. Rayner, and Emmanuel Benichou†

Steacie Institute for Molecular Sciences, National Research Council of Canada,100 Sussex Drive, Ottawa, Ontario, Canada K1A 0R6

Norma Mireles, Francisco J. Tenorio, and Ana Martínez

Instituto de Investigaciones en Materiales, UNAM.Circuito Exterior s/n, Ciudad Universitaria, 04510 Coyoacán, México, D.F.

Received: June 30, 2003; In Final Form: August 30, 2003

The reactivity of the yttrium atom toward ammonia at room temperature has been investigated in a fast-flow reactor. The first step in the reaction is the rapid formation of yttrium imide (YNH) through the oxidative addition of the N−H bond of ammonia and the elimination of molecular hydrogen. The reaction continues with the solvation of yttrium imide with up to three molecules of ammonia. An equilibrium is established between the $YNH(NH_3)_2$ and $YNH(NH_3)_3$ species. The binding energy of NH_3 in the $YNH(NH_3)_3$ complex is found to be 19.7 ± 0.3 kcal/mol. Reaction rates have been determined for the solvation processes. Density functional calculations indicate that up to four ammonia molecules can bind to YNH at 0 K. The calculated D_e is highest for the YNH−NH_3 complex and decreases abruptly following the addition of the third ammonia molecule. The calculated binding energy of the $YNH(NH_3)_3$ complex is 12 kcal/mol, in fair agreement with experiment. The $YNH(NH_3)_4$ complex is too weakly bound to be observed in our experiment. The structures of the complexes have been determined through full geometry optimizations. A molecular orbital analysis indicates that ammonia molecules are ligated to the positive end (Y) of the large dipole of YNH through dipole−dipole interactions and dative bond formation. The singly occupied sp hybrid on Y forces the ammonia molecules to bind side-on to Y.

I. Introduction

Solvation involves the formation of molecular complexes resulting from the binding of molecules on a species. It occurs each time a molecule becomes imbedded into a solvent. Solvation is in many respects the first intimate act between reacting partners and defines the spatial position of molecules before reacting, if reaction is going to occur. A simple way to investigate solvation is to study isolated molecule/solvent complexes in the gas phase. We are interested in solvation of metal centers such as atoms, unsaturated metal complexes, and clusters by small molecules. We believe that such studies contribute to the development of a molecular understanding of physisorption and chemisorption on metal surfaces as well as the chemistry of metal centers in solution.

This paper focuses on the interaction of yttrium atoms with ammonia. Transition metal atoms and clusters exhibit different bonding behavior with ammonia. Siegbahn et al. investigated theoretically the oxidative addition of the N−H bond of ammonia onto second-row transition metal atoms.[1] They reported the formation of an M−NH_3 molecular complex before the oxidative addition occurs. For Y, Zr, and Nb, the adduct formation is exothermic and no activation barrier is found for the oxidative addition of the N−H bond. The adducts result from the donation of the ammonia lone pair electrons into the empty d-orbital of the metal atom. A recent theoretical investigation of the reaction $Y^+ + NH_3$ by Ye and Dai shows that the reaction proceeds through the formation of the adduct followed by the oxidative addition of the N−H bond.[2] The exothermicity of the reaction $Y^+ + NH_3 \rightarrow H-Y-NH_2^+$ is large enough to overcome the small activation barrier of 11 kcal/mol, necessary to form $YNH^+ + H_2$ products. Presumably, this also happens with neutral yttrium atoms, but this has never been proven experimentally. It is known that yttrium imide is formed readily when ammonia is introduced in the plasma resulting from the laser vaporization of yttrium, but this may result from ion, excited states, or high-temperature chemistry.[3,4] Here, we demonstrate that indeed neutral yttrium atoms thermalized at 300 K react with ammonia to produce YNH. In addition, we show that further interactions with ammonia lead to the solvation of YNH rather than additional oxidative addition. In particular, up to three ammonia molecules can be added to YNH at room temperature. Why the solvation process stops at three molecules is intriguing. Also, what are the structures and binding energies of these systems, and what is the nature of the bonding? This paper provides answers to these questions through density functional calculations. These types of systems are held together by relatively weak bonds and hence offer benchmarks to computational methods. Here, we demonstrate that density functional theory (DFT) performs relatively well on these weakly bond systems and together with experimental data provides deep insights into these challenging systems.

II. Experimental Procedure

The experiment combines a Smalley-type metal cluster source, fast-flow reactor, and a reflectron time-of-flight mass

† Current address: Laboratoire de Spectrométrie Ionique et moléculaire, U.M.R. C.N.R.S. 5579, Bâtiment Alfred Kastler, Domaine Scientifique de la Doua, Université Claude Bernard-Lyon 1, 43 bd du 11 Novembre 1918, 69622 Villeurbanne cedex, France.

* To whom correspondences should be addressed: e-mail Benoit.Simard@nrc-cnrc.gc.ca; phone (613) 990-0977; FAX (613) 991-2648.

10.1021/jp035871k CCC: $25.00
Published on Web 10/04/2003

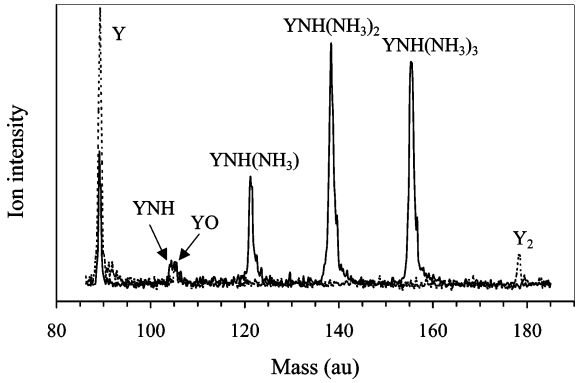

Figure 1. Reaction of yttrium atom with ammonia: time-of-flight spectra obtained respectively without ammonia (dash line) and with 0.01% of ammonia in the reactor (solid line).

spectrometer (R-TOFMS). The experimental setup has been described in detail previously.[5] Briefly, the yttrium atoms were produced in a Smalley-type laser vaporization source. A pulsed laser beam (XeCl excimer, 10 Hz, 30 mJ) was focused onto a yttrium rod (99.9% pure from Alfa products). The atoms were entrained by a continuous flow of helium. A mass flow controller (MKS, Canada) maintained this He flow to 15000 sccm (standard cubic centimeters per minute). Reagent gas (mixture of NH_3 (1%) and He (99%)) was added through an inlet ring positioned 60 cm from the source and 70 cm upstream of the sampling point. The reagent flow was set in the range 0−200 sccm by using a mass flow controller. The temperature and the pressure in the reactor were regulated ($261 < T < 373$ K and $0.4 < P < 2$ Torr). Variation of the pressure changes the velocities of the clusters and, thus, the contact time with the reagent. A pulsed shutter was used to reduce the gas load in the differentially pumped chamber between the flow tube (0.4−2 Torr) and the RTOFMS (10^{-7}−10^{-6} Torr), the bulk of the carrier gas being evacuated by a mechanical booster pump. Reaction products were ionized by a pulsed ArF laser (193 nm, 10 Hz) at low fluence (less than 500 μJ/pulse). Ions were mass selected and detected by microchannel plates.

III. Computational Details

All calculations were performed using Gaussian 94 and the Becke's 1988 functional, which includes the Slater exchange along with the corrections involving the gradient of the density, with Perdew and Wang's 1991 gradient-corrected correlation functional (BPW91).[6−8] These calculations were carried out with LANL2DZ atomic orbital basis functions.[9−11] Full geometry optimization without symmetry constraints has been performed, starting from several initial geometries to locate different minima on the potential energy surface. Different spin multiplicities ($2S + 1$) were considered in all calculations in order to find the most stable spin state. To find the global minimum, one must consider several multiplicities and several initial structures for each adduct. The possibility that the true global minimum was missed in the optimization procedure cannot be excluded, but the number of different initial geometries and spin multiplicities that were considered is sufficiently high to feel confident that the global minimum has been identified.

IV. Results and Analyses of Experimental Data

Figure 1 shows a time-of-flight mass spectrum in the mass range covering the yttrium atom and the yttrium dimer obtained without (dashed line) and with 0.03% of ammonia (solid line) at room temperature and at a total pressure of 2 Torr. The addition of ammonia rapidly titrates the yttrium atoms to produce yttrium imide (YNH), which is itself titrated away to form yttrium imide−ammonia complexes with up to three ammonia molecules, $YNH(NH_3)_{1,2,3}$. No higher complexes are observed. Previous experiments have shown that only association complexes with binding energies larger than about 10 kcal/mol survive in detectable quantities in our flow tube apparatus at room temperature (ref 5 and references therein). This provides a lower bound for the binding energies of the complexes observed. The absence of higher complexes is attributed to either small or negligible binding energies. As will shown below, our calculations predict that $YNH(NH_3)_4$ is stable, but the binding energy is close if not below the observation threshold of 10 kcal/mol. Our calculations also predict that a fifth ammonia molecule cannot be added.

TABLE 1: Bond Angles (deg) and Ionization Potentials (eV)

species	bond angles	exptl IP	calcd IP
YNH	Y−NH = 180	5.839	5.76
$YNH(NH_3)$	HN−Y−NH_3 = 93	<5.8	4.87
$YNH(NH_3)_2$	HN−Y−NH_3 = 92 H_3N−Y−NH_3 = 173	<5.8	4.12
$YNH(NH_3)_3$	HN−Y−NH_3 = 83, 96, 98 H_3N−Y−NH_3 = 87, 128, 144	<5.8	3.20
$YNH(NH_3)_4$	HN−Y−NH_3 = 98, 100, 102 H_3N−Y−NH_3 = 88	*a*	2.68

[a] Not observed.

The ionization energies of all the species are smaller than the photon energy of the ionization laser. This means that the species are ionized by a one-photon transition and that the ion signal intensity is proportional to the concentration of the corresponding species. However, the ionization cross sections differ from species to species and become larger with successive addition of ammonia. This is reflected in the lowering of the ionization potential with successive addition of ammonia. Experimental and theoretical values for the ionization potentials are given in Table 1. The yttrium content of the species originates from the reaction of yttrium atoms with ammonia. If the species had the same cross sections, the sum of the signal intensities of the products would be the same as the intensity drop of the yttrium atomic ion signal. This is not the case. However, it is possible to estimate relative ionization cross sections through mass balance (see below). The depletion of yttrium atom by ammonia followed by the subsequent growth and decay of products is modeled here using the following pseudo-first-order kinetic consecutive reaction scheme:

$$Y + NH_3 \xrightarrow{k_1} YNH + H_2 \quad (1)$$

$$YNH + NH_3 \xrightarrow{k_2} YNH(NH_3) \quad (2)$$

$$YNH(NH_3) + NH_3 \xrightarrow{k_3} YNH(NH_3)_2 \quad (3)$$

$$YNH(NH_3)_2 + NH_3 \underset{k_{-4}}{\overset{k_4}{\rightleftarrows}} YNH(NH_3)_3 \quad (4)$$

Under pseudo-first-order conditions, these yield a series of linked differential equations, describing the growth and decay of the reactants and products, which when solved give the relative concentrations $[Y]/[Y]_{t=0}$, $[YNH]/[Y]_{t=0}$, $[YNH(NH_3)]/[Y]_{t=0}$, $[YNH(NH_3)_2]/[Y]_{t=0}$, and $[YNH(NH_3)_3]/[Y]_{t=0}$.

The results for the first three consecutive reactions are

$$\frac{[Y]}{[Y]_0} = \exp(-k_1[NH_3]t) \quad (5)$$

$$\frac{[YNH]}{[Y]_0} = \frac{k_1}{k_2 - k_1}(\exp(-k_1[NH_3]t) - \exp(-k_2[NH_3]t)) \quad (6)$$

$$\frac{[YNH(NH_3)]}{[Y]_0} = \frac{k_1k_2}{(k_2 - k_1)(k_3 - k_1)(k_3 - k_2)}[(k_3 - k_2)\exp(-k_1[NH_3]t) - (k_3 - k_1)\exp(-k_2[NH_3]t) + (k_2 - k_1)\exp(-k_3[NH_3]t)] \quad (7)$$

By fitting the experimental data to eqs 5−7, it is possible to determine successively the values of k_1, k_2, and k_3 (see Figure 2). To do such a fit, we have plotted the ratio [species]/$[Y]_{t=0}$ as a function of the product $[NH_3]\tau$ (where τ is the contact time with ammonia). An absolute value of the rate constant, k_1, for the depletion of yttrium can be obtained readily by fitting the $[I(Y)]/[I(Y)_{t=0}] = [Y]/[Y]_0$ ratio to eq 5. Figure 2 shows this fit for which a value of $k_1 = (1.1 \pm 0.2) \times 10^{-11}$ cm^3 s^{-1} is obtained. This value can then be used in eq 6 to determine k_2, which in turn can be used in eq 7 to determine k_3. The derived rate constants are $k_2 = (8.0 \pm 1.0) \times 10^{-11}$ cm^3 s^{-1} and $k_3 = (7.3 \pm 2.1) \times 10^{-11}$ cm^3 s^{-1}. To arrive at these values, the data had to be corrected for the different ionization cross sections (vide supra). Relative ionization efficiencies were determined by fitting the normalized sum of relative concentration $\sum(I(x)/I[Y]_0)$, x = Y, YNH, $YNH(NH_3)$, $YNH(NH_3)_2$, and $YNH(NH_3)_3$, to unity at all points.

The measured kinetics of $YNH(NH_3)_2$ and $YNH(NH_3)_3$ are not consistent with irreversible conversion of $YNH(NH_3)_2$ to $YNH(NH_3)_3$. It is necessary to consider an equilibrium reaction between $YNH(NH_3)_2$ and $YNH(NH_3)_3$. This is indicated in reaction 4. The resulting coupled differential equations lead to

$$\frac{[YNH(NH_3)_2]}{[Y_0]} = a_1a_2a_3\sum_{i=0}^{4}\frac{a_i - k_4}{q'(a_i)}e^{-a_it} \quad (8)$$

$$\frac{[YNH(NH_3)_2]}{[Y_0]} = a_1a_2a_3k_4[NH_3]\sum_{i=0}^{4}\frac{1}{q'(a_i)}e^{-a_it} \quad (9)$$

where $a_0 = 0$, $a_1 = k_1[NH_3]$, $a_2 = k_2[NH_3]$, $a_3 = k_3[NH_3]$, $a_4 = (k_4[NH_3] + k_{-4})$, and $q'(a_i) = \prod_{j\neq i}(a_i - a_j)$. Because τ and $[NH_3]$ are independent variables, we have plotted the experimental data only as a function of $[NH_3]$ for three different contact times (τ = 9, 12, and 22 ms, corresponding to three different pressures respectively P = 0.7, 1, and 2 Torr). These plots are presented in Figure 3. Fitting these data to eqs 8 and 9 permits the determination of k_4 and k_{-4}. The large uncertainty on the individual values is large. However, the values are highly correlated, and their ratio, k_4/k_{-4} (i.e., the equilibrium constant K), can be determined with reasonable uncertainty. We applied the fitting procedure to the experimental data on the two species $YNH(NH_3)_2$ and $YNH(NH_3)_3$ at three different pressures (see Figure 3) and obtained a reliable value of $K = (1.4 \pm 0.6) \times 10^7$ atm^{-1} for the equilibrium (dissociation) constant at 300 K.

This measurement of the equilibrium constant at 300 K can be used to derive the binding energy using the statistical

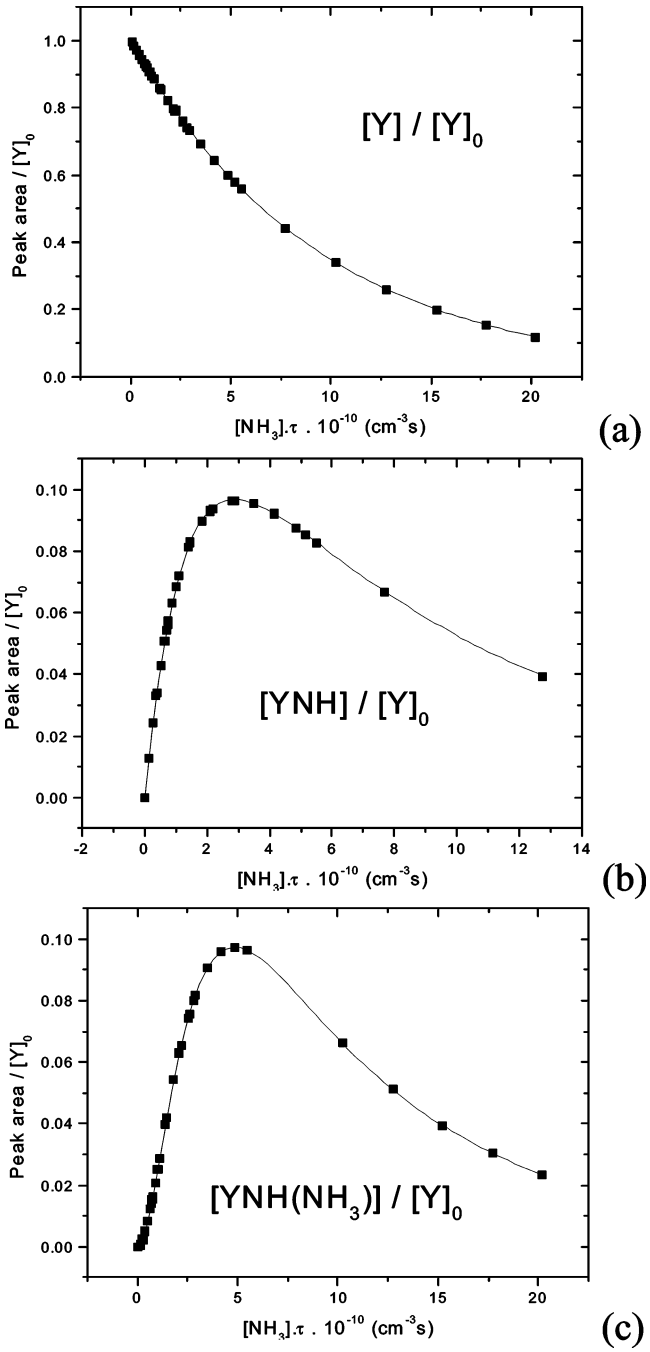

Figure 2. Variation in the peak area (concentration) of Y (a), YNH (b), and $YNH(NH_3)$ (c) with the product of the ammonia concentration and the contact time. The solid lines represent the fit of the experimental data with eqs 5−7.

mechanics relationship (third-law method)

$$K_p = \frac{1}{N}\frac{Q_{YNH(NH_3)_3}}{Q_{NH_3}Q_{YNH(NH_3)_2}}e^{E_0/kT} \quad (10)$$

where Q is the partition function. These functions were determined from the DFT calculated structures and vibrational frequencies (Table 2), yielding a binding energy $\Delta E_{300} = 19.7 \pm 0.3$ kcal mol^{-1} for the $YNH(NH_3)_3$ complex. The quoted error is that arising from experimental error in K_p. Errors associated with the partition functions are expected to be small. The partition function term is dominated by the loss of three translational degrees of freedom. The binding entropy is derived to be $\Delta S°_{300} = -34$ cal mol^{-1} K^{-1}.

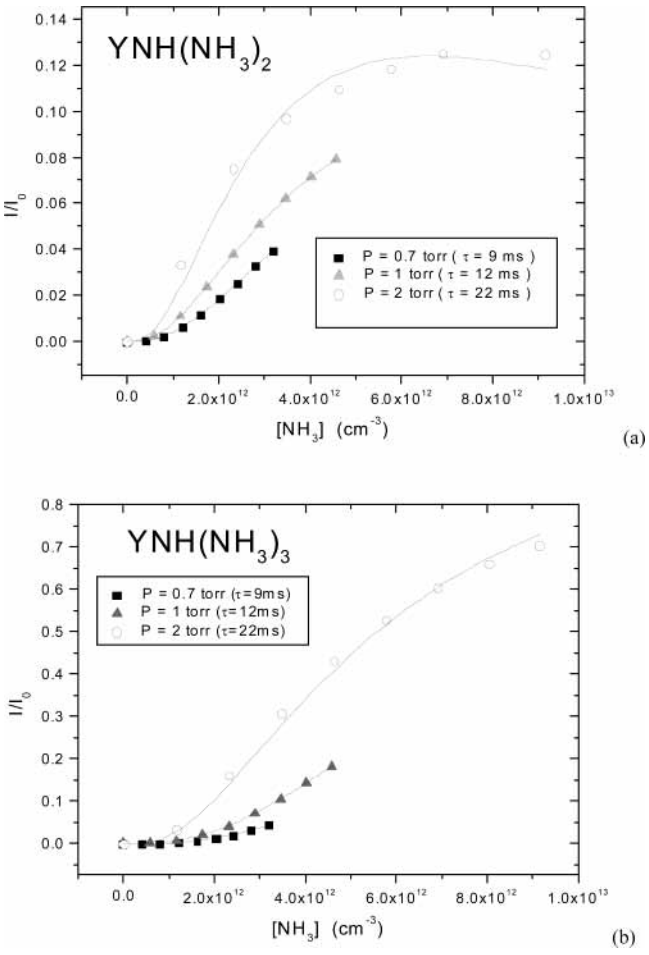

Figure 3. Variation in the peak area (concentration) of $YNH(NH_3)_2$ (a) and $YNH(NH_3)_3$ (b) with the ammonia concentration for three different contact times (i.e., three different pressures in the reactor P = 0.7, 1, and 2 Torr). The solid lines represent the fit of these data obtained with eqs 8 and 9.

TABLE 2: Calculated Harmonic Frequencies (in cm^{-1}) of the Complexes

YNH		592	843	3461		
$YNH(NH_3)$	42	111	302	465	547	565
	587	808	1132	1636	1657	3334
	3441	3502	3527			
$YNH(NH_3)_2$	38i	23	43	69	92	279
	301	405	432	495	509	547
	568	773	1041	1054	1633	1633
	1654	1655	3329	3333	3426	3509
	3511	3542	3546			
$YNH(NH_3)_3$	36i	28	70	76	80	89
	129	185	257	272	308	352
	429	464	487	529	579	582
	599	742	1018	1057	1063	1620
	1623	1627	1631	1639	1646	3146
	3268	3295	3417	3458	3463	3490
	3503	3525	3565			
$YNH(NH_3)_4$	41	41	59	71	76	80
	84	88	94	111	117	253
	269	277	279	349	359	370
	481	489	496	506	549	600
	602	738	1024	1028	1036	1044
	1614	1617	1627	1631	1635	1637
	1643	1645	3234	3258	3261	3284
	3405	3449	3454	3472	3478	3501
	3504	3514	3515			

V. Results and Analyses of Computational Data

Figure 4 shows the optimized geometries for the most stable structures that were considered. For YNH, the Y−N bond distance is 1.89 Å. This bond distance becomes larger when the ammonia molecules are involved. In general, the Y−N distance increases when one goes from the complex with one ammonia molecule to the cluster with four ammonia subunits. The Y−N distances are almost the same for three and four ammonia molecule cases. For all the structures presented in the figure, the Y−NH distance is shorter than the Y−NH_3 bond length. The structures are minima on the potential energy surfaces. For $YNH(NH_3)_2$ and $YNH(NH_3)_3$, one imaginary frequency was found (equal to 38i and 36i cm^{-1}, respectively; see Table 2). Similar results were reported by Mierzwicki et al. for the Li atom and Hashimoto et al. for $Na(NH_3)_2$ and $Na(NH_3)_3$ complexes, where NH_3 molecules could rotate almost freely around the M−N bonds.[12,13] The imaginary frequency of $YNH(NH_3)_2$ and $YNH(NH_3)_3$ that we found also corresponds to the rotation of the NH_3 molecule around the Y−NH_3 bond. Therefore, it is safe to assume that the geometries presented in Table 4, and the energies of these structures are quite similar to the minima on the potential energy surface.

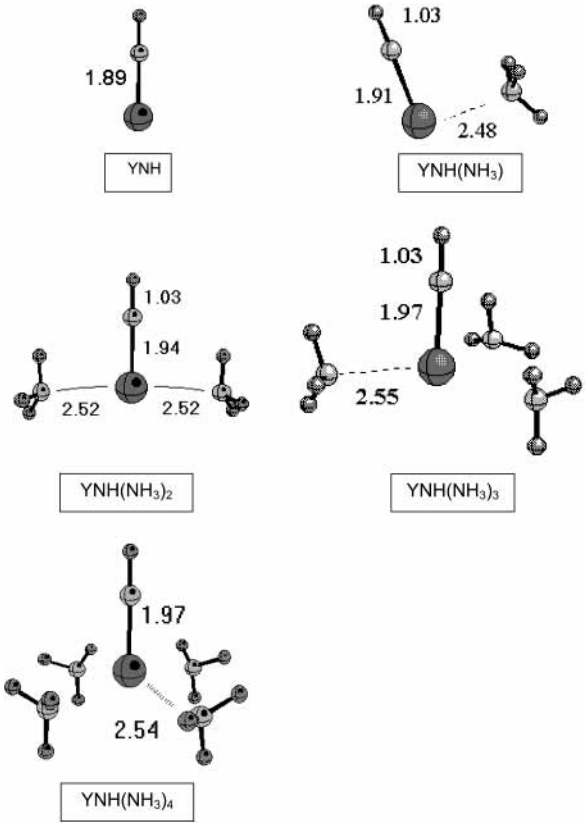

Figure 4. Optimized structures of $YNH(NH_3)_x$. The geometries were obtained at GGA level (BPW91)[15] and LANDL2DZ.[16]

Table 3 reports the net atomic charges from Mulliken population analyses. The analysis of the YNH compounds with ammonia shows that there is a charge-transfer process from the Y atom to the NH moiety. There is also a charge transfer from the NH_3 molecule to the Y atom, suggestive of a dative bond formation. Thus, the Y atom becomes less positive with increasing number of ammonia molecules. As can be seen in Table 3, the atomic charge on the ammonia molecules decreases as the number of ammonia molecule increases. The analysis of the bond distances shows that the charge-transfer process from NH_3 to Y weakens the Y−NH bond. As a consequence, the Y−NH bond is shorter when no ammonia molecules are present.

The binding energies for the $YNH(NH_3)_{n-1} + NH_3 \rightarrow YNH(NH_3)_n$ reaction are reported in Table 4. In all cases, the products of the reaction are more stable than the reactants. For $YNH(NH_3)$, the binding energy is larger than the binding energy with two, three, or four ammonia molecules. Clearly, it is more

TABLE 3: Net Atomic Charges from Mulliken Population Analysis for $YNH(NH_3)_n$ with $n = 0, 1, 2, 3, 4$

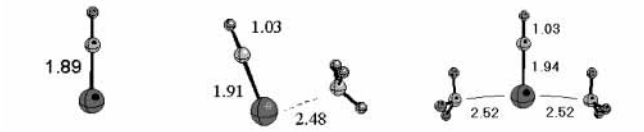

Net atomic charges	Net atomic charges	Net atomic charges
Y = 0.38 NH = -0.38 N of NH = -0.62	Y = 0.26 NH = -0.43 NH_3 = 0.17 N of NH = -0.65 N of NH_3 = -0.91	Y = 0.20 NH = -0.49 NH_3 = 0.15 N of NH = -0.70 N of NH_3 = -0.91

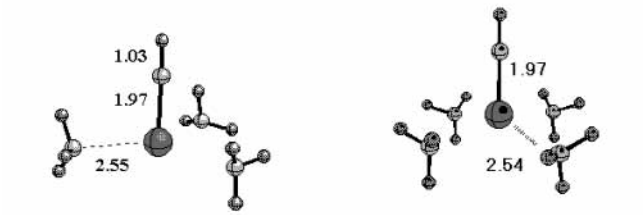

Net atomic charges	Net atomic charges
Y = 0.11 NH = -0.54 NH_3 = 0.14 N of NH = -0.74 N of NH_3 = -0.90	Y = 0.07 NH = -0.52 NH_3 = 0.11 N of NH = -0.71 N of NH_3 = -0.89

TABLE 4: Reaction Energies (kcal/mol) for $YNH(NH_3)_{n-1} + NH_3 \rightarrow YNH(NH_3)_n$

reaction	ΔE (kcal/mol)
$YNH + NH_3 \rightarrow YNH(NH_3)$	−21.53
$YNH(NH_3) + NH_3 \rightarrow YNH(NH_3)_2$	−20.79
$YNH(NH_3)_2 + NH_3 \rightarrow YNH(NH_3)_3$	−12.30
$YNH(NH_3)_3 + NH_3 \rightarrow YNH(NH_3)_4$	−10.73

favorable to add one ammonia molecule to YNH than to the system that already has three ammonia molecules. It appears that for YNH there is a relation between the atomic charge and the binding energy; namely, as the atomic charge of the Y atom increases, the binding energy also increases. This suggests that there is a dipole−dipole contribution to the binding.

The general appearance of the molecular orbitals (see Supporting Information) is quite similar for all of the systems. The highest occupied molecular orbital (HOMO) is a nonbonding 5s5p hybrid orbital of the Y atom. In addition, there are two π bonding and one σ bonding orbitals between Y and NH. The energies of these orbitals are quite similar for all the systems. Hence, the covalent Y−NH bond is not affected significantly by the presence of ammonia molecules.

There is no molecular orbital that can be associated with a purely covalent bond between the ammonia molecules and YNH. For $YNH(NH_3)$ it is possible to find three nonbonding NH_3 molecular orbitals: two degenerate at −0.48 au and one at −0.30 au. The situation is quite similar for $YNH(NH_3)_2$. Six nonbonding NH_3 molecular orbitals are found: four orbitals at −0.45 au and two at −0.27 au. With three ammonia molecules, nine nonbonding NH_3 molecular orbitals are found (−0.45 and −0.27 au) while for $YNH(NH_3)_4$ 12 nonbonding NH_3 molecular orbitals result. The energies of the nonbonding NH_3 molecular orbitals are quite similar for the four systems. In all cases, we found three nonbonding molecular orbitals for each ammonia molecule. The character of the Y−NH bond remains the same, no matter how many ammonia molecules are added.

VI. Discussion

Previous theoretical studies had given the following incomplete picture of the reaction between neutral yttrium atoms and ammonia.[1,14] The reaction begins with the formation of a $Y-NH_3$ adduct. This complexation is exothermic by about 20 kcal/mol. The adduct results from the donation of the ammonia lone pair into the empty d orbitals of yttrium. However, the adduct is unstable, and as there is no activation barrier, the insertion occurs readily to form the $H-Y-NH_2$ intermediate, a planar molecule. The calculations did not go beyond this intermediate, but from the reaction $Y^+ + NH_3$ studied theoretically by Ye and Dai, it was believed that the exothermicity is high enough to overcome any barriers, and this would lead to a rapid 1−2 H_2 loss to form yttrium imide.[2] This study proves unequivocally that the primary product of the reaction between thermalized neutral yttrium atoms and ammonia is yttrium imide and supports the previous theoretical findings that there is no activation barrier for the insertion of yttrium into the N−H bond.

It is interesting to realize that the binding of the imide radical onto the yttrium atom neutralizes the capacity of that yttrium atom to activate the N−H bond of other ammonia molecules. Rather, the yttrium moiety prefers to be solvated by the ammonia molecules. The bonding, which is relatively weak, arises from two contributions. There is an electrostatic dipole−dipole contribution, which likely acts at long range to align the negative end of the dipole of ammonia, the lone pair, to the positive end of the yttrium imide dipole. As the ammonia molecules get closer to the yttrium moiety, weak dative bonds, in which ammonia transfers electron density, are formed. This electron donation from ammonia to empty hybrid orbitals of yttrium is the second contribution to the bonding. If the electrostatic dipole−dipole interaction were the only contribution to the bonding, ammonia would also solvate the hydrogen atom of the NH moiety because, like Y, it is also positively charged. The reason why this does not occur is because of the lack of empty accepting orbitals on H. The two contributions appear to counteract each other. As electron density is given to the yttrium moiety, the positive charge on Y decreases, thus reducing the dipole−dipole contribution. This is why the binding energy decreases with the number of solvating ammonia molecules. The positive charge reduction on Y also weakens the Y−NH bond, which gets longer with the number of solvating ammonia molecules.

One may wonder why ammonia is solvating yttrium from the side of YNH rather than end-on along the internuclear axis of YNH. The answer is simple. The HOMO of YNH, the nonbonding 5s5p hybrid orbital projecting out of the Y−N−H axis, is singly occupied. Stark experiments conducted in our laboratory, which established the permanent dipole moment of YNH as 3.33 ± 0.07 D, indicate that the hybridization moment of the 12σ orbital is about 1.2 D.[15] This is the moment resulting from the charge separation between the positive Y atom and the singly occupied 12σ orbital.[16] Clearly, this is enough to prevent any solvation from that end.

The solvation of ammonia around the yttrium atom of YNH is made possible by availability of empty orbitals on Y. Two Y 4d orbitals are used to make the two bonds in YNH. This leaves three empty 4d orbitals along with the 5s and 5p orbitals. All of these orbitals are very close in energy. It is interesting to note that the geometries of the complexes are very much like those one would have predicted from the simple valence shell electron pair repulsion (VSEPR) model. The ammonia molecules lie essentially at 90° from the YNH axis. The $H_3N-Y-NH_3$ angle is essentially 180°, 120°, and 90° in the $YNH(NH_3)_2$,

$YNH(NH_3)_3$, and $YNH(NH_3)_4$ complex, respectively (see Table 1). Therefore, the corresponding overall geometries are T-shaped, trigonal pyramidal, and square pyramidal. Obviously, the bonds are not all equivalent. The Y−NH bond is much stronger. Thus, it is not appropriate to associate a particular orbital hybridization for the whole system. The weakening of the Y−N bond upon successive addition of ammonia may be viewed as a tendency for the systems to equilibrate the bond toward a unique hydridization. The strength of the bonds in YNH prevents solvation by more than four ammonia molecules. Adding a fifth ammonia molecule to produce a pentagonal bipyramid geometry would require too major a change in the bonding structure of YNH for the system to be stable, and indeed our calculations indicate that it is not possible to add a fifth ammonia molecule.

The binding energies are all relatively small. Thus, one may wonder whether the DFT method used leads to appropriate description of the systems. One checkpoint is the binding energies. As mentioned before, complexes with binding energy larger than about 10 kcal/mol are observable in our flow-tube apparatus. Since the $YNH(NH_3)_4$ complex is not observed in our experiment, its binding energy must be less than about 10 kcal/mol. This is the value that we calculated for this complex. The binding energy, D_e, of the $YNH(NH_3)_3$ complex is calculated to be 12 kcal/mol, about $^2/_3$ the experimental D_0 value of 20 kcal/mol. This indicates that the binding energies reported herein are underestimated by as much as 30%. The calculated structures should be reliable, however.

VII. Conclusion

An experimental and theoretical study of the solvation of an yttrium atom with ammonia has been reported. Yttrium atoms thermalized at room temperature activate readily the N−H bond of ammonia. The oxidative addition proceeds without activation barrier, and the exothermicity is high enough to yield readily yttrium imide through the elimination of molecular hydrogen. The yttrium imide molecule is chemically inert toward ammonia. The molecule becomes solvated by up to four ammonia molecules, which weakly bind to yttrium perpendicularly to the YNH axis. The ammonia molecules align in a plane perpendicular to the YNH axis to minimize the electron repulsion in accord with the simple VSEPR model. The binding arises from two counteracting contributions: electrostatic dipole−dipole interaction and dative interaction.

Supporting Information Available: Molecular orbital pictures for $YNH(NH_3)$, $YNH(NH_3)_2$, $YNH(NH_3)_3$, and $YNH(NH_3)_4$. This material is available free of charge via the Internet at http://pubs.acs.org.

References and Notes

(1) Blomberg, M. R. A.; Siegbahn, P. E. M.; Svensson, M. *Inorg. Chem.* **1993**, *32*, 4218.
(2) Ye, S.; Dai, S. *Int. J. Quantum Chem.* **1996**, *59*, 421.
(3) Simard, B.; Jakubek, Z. J.; Niki, H.; Balfour, W. J. *J. Chem. Phys.* **1999**, *111*, 1483.
(4) Jakubek, Z. J.; Simard, B.; Niki, H.; Balfour, W. J. *J. Chem. Phys.* **2000**, *113*, 3591.
(5) Simard, B.; Mitchell, S. A.; Rayner, D. M.; Yang, D. S. In *Metal−Ligand Interactions in Chemistry, Physics and Biology*; Russo, N., Salahub, D. R., Eds.; Kluwer Academic Publishers: Dordrecht, The Netherlands, 2000; pp 239−294.
(6) Frisch, M. J.; Trucks, G. W.; Schlegel, H. B.; Gill, P. M. W.; Johnson, B. G.; Robb, M. A.; Cheeseman, J. R.; Keith, T. A.; Peterson, G. A.; Montgomery, J. A.; Raghavachari, K.; Al-Laham, M. A.; Zakrzewski, V. G.; Ortiz, J. V.; Foresman, J. B.; Cioslowski, J.; Stefanov, B. B.; Nanayakkara, A.; Challacombe, M.; Peng, C. Y.; Ayala, P. Y.; Chen, W.; Wong, W. M.; Andrés, J. L.; Replogl, E. S.; Gomperts, R.; Martin, R. L.; Fox, D. J.; Binkley, J. S.; Defrees, D. J.; Baker, J.; Stewart, J. P.; Head-Gordon, M.; Gonzalez, C.; Pople, J. A. *Gaussian 94*, Revision D.4; Gaussian Inc.: Pittsburgh, PA, 1995.
(7) Becke, A. D. *Phys. Rev. A* **1988**, *38*, 3098.
(8) Perdew, J. P.; Wang, Y. *Phys. Rev. B* **1992**, *45*, 13244.
(9) Hay, P. J.; Wadt, W. R. *J. Chem. Phys.* **1985**, *82*, 270.
(10) Wadt, W. R.; Hay, P. J. *J. Chem. Phys.* **1985**, *82*, 284.
(11) Hay, P. J.; Wadt, W. R. *J. Chem. Phys.* **1985**, *82*, 299.
(12) Mierzwicki, Z.; Latajka, K. *Chem. Phys.* **2001**, *265*, 301.
(13) Hashimoto, K.; Kamimoto, T. *J. Am. Chem. Soc.* **1998**, *120*, 3560.
(14) Tsipis, A. C. *J. Chem. Soc., Faraday Trans.* **1998**, *94*, 11.
(15) Simard, B., to be published.
(16) Gordy, W.; Cook, R. L. *Microwave Molecular Spectra*; Wiley: New York, 1984; p 784 ff.